Modelling the global efficiency of dissolved air flotation

D.M. Leppinen*, S.B. Dalziel* and P.F. Linden**

*Department of Applied Mathematics and Theoretical Physics, University of Cambridge, Silver Street, Cambridge CB3 9EW, UK

**Department of Mechanical and Aerospace Engineering, University of California, San Diego, 9500 Gilman Drive, La Jolla CA 92093-0411, USA

Abstract The purpose of this paper is to examine how the efficiency of dissolved air flotation is affected by the size of bubbles and particles. The rise speed of bubble/particle agglomerates is modelled as a function of bubble and particle size, while the kinematics of the bubble attachment process is modelled using the population balance approach adopted by Matsui, Fukushi and Tambo. It is found that flotation, in general, is enhanced by the use of larger particles and larger bubbles. In particular, it is concluded that for the ultra-high surface loading rates of 25 m/hr or more planned for future flotation tanks, bubble size will have to be increased by a factor of two over the size currently employed in many facilities during dissolved air flotation.
Keywords Dissolved air flotation; efficiency; population balance model

Water Science and Technology **Vol 43 No 8 pp 159–166** © IWA Publishing 2001

Introduction

In many countries dissolved air flotation (DAF) is replacing sedimentation as the process of choice for the pre-filtration stage of potable water treatment. Water sources often contain light or almost neutrally buoyant particles which are not efficiently removed by sedimentation. The objective of DAF is to attach bubbles onto the surface of particles to form positively buoyant bubble/particle agglomerates. These agglomerates rise to the top of the flotation tank and are incorporated into a foam layer that can subsequently be skimmed off. DAF has the advantage over sedimentation of being able to operate at higher surface loading rates (volumetric flow rate divided by surface area of tank) since the rise speed of bubble/particle agglomerates can be much larger than the settling speed of individual particles. Consequently DAF tanks can be designed with smaller surface areas, or larger flow rates, than sedimentation tanks, resulting in substantial capital savings. Current DAF tanks typically operate at surface loading rates of between 3–12 m/hr (O'Neill *et al.*, 1997). Ultra-high flow rate flotation tanks with flow rates as high as 25 m/hr are currently being designed (Shawcross *et al.*, 1997) and it is expected that even higher surface loading rates will be achieved in the future. This paper examines the influence of bubble and particle size on the overall efficiency of the flotation process as the surface loading rate is varied. The maximum rise velocity of bubble/particle agglomerates is modelled as a function of bubble and particle size and a kinematic model is used to examine the formation of bubble/particle agglomerates within the contact zone of a DAF tank. The influence of varying bubble and particle sizes is examined and the implications for maximizing the particle removal efficiency of DAF are outlined.

Rise speed of bubble/particle agglomerates

The rise speed of bubble/particle agglomerates can be very different from the rise speed of individual DAF bubbles, and thus it is essential to be able to estimate the rise speed of these agglomerates. In what follows, it is assumed that the particles to be removed by flotation can be approximated as spheres with diameter d_p and density ρ_p and that the bubbles are spherical with diameter d_b and density ρ_b. Since the number density of bubbles in a typical

DAF system greatly exceeds the number density of particles, it is assumed that a bubble/particle agglomerate will be comprised of a single particle and an integer number, *i*, of bubbles and that the agglomerate will have the same rise speed as a solid sphere with equivalent volume and density. This approximation neglects the non-sphericity of the agglomerates, which is reasonable for cases where the particles are much larger than the bubbles. This approximation also neglects the surface mobility of the bubbles, which again is reasonable since the surface mobility is restricted due to contact with the particle and due to the influence of surfactants.

The equivalent diameter and density of a sphere with the same total volume and mass of a bubble/particle agglomerate comprised of one particle and *i* bubbles are calculated as

$$d_{equiv}^3 = \left(d_p^3 + i d_b^3\right)^3 \quad \text{and} \quad \rho_{equiv} = \left(\rho_p d_p^3 + i\rho_b d_b^3\right) / \left(d_p^3 + i d_b^3\right). \tag{1}$$

The total buoyancy force acting on the bubble / particle agglomerate is

$$F_{Buoyancy} = \pi d_{equiv}^3 \left(\rho - \rho_{equiv}\right) g / 6 \tag{2}$$

where ρ is the density of water and *g* is the acceleration due to gravity. The rise speed, v_i, of an agglomerate with *i* bubbles is determined by equating the buoyancy force acting on the agglomerate with the steady drag force acting on the equivalent solid sphere translating at the same speed. The drag force, F_{Drag}, acting on the equivalent sphere can readily be calculated as a function of its speed through known correlations of the sphere's drag coefficient, C_D, as a function of the sphere's Reynolds number, Re:

$$C_D = \frac{F_{Drag}}{\pi\rho v_i^2 d_{equiv}^2 / 8} = f\left(\mathrm{Re} = \frac{\rho v_i d_{equiv}}{\mu}\right) \tag{3}$$

where *f*(Re) is a known function of the Reynolds number and μ is the dynamic viscosity of water. The rise speed of the sphere is given by substituting $F_{Buoyancy} = F_{Drag}$ into (3) yielding

$$v_i = \left(\frac{F_{Buoyancy}}{f(\mathrm{Re})\pi\rho d_{equiv}^2 / 8}\right)^{1/2}. \tag{4}$$

The drag function correlation recommended by Clift *et al*. (1978) is

$$f(\mathrm{Re}) = \begin{cases} \dfrac{24}{\mathrm{Re}}\left(1 + \frac{3}{16}\mathrm{Re}\right) & \mathrm{Re} < 0.01 \\ \dfrac{24}{\mathrm{Re}}\left(1 + 0.1315\,\mathrm{Re}^{0.82 - 0.05\log_{10}\mathrm{Re}}\right) & 0.01 \le \mathrm{Re} \le 20 \end{cases} \tag{5}$$

where it is noted that during DAF, Re is typically of *O*(1) or smaller. The rise speed is determined by solving (3) to (5) in an iterative fashion, starting with the Stokes approximation

$$v_i = \frac{\left(\rho - \rho_{equiv}\right) g d_{equiv}^2}{18\mu} \tag{6}$$

which corresponds to the limit of Re→0.

Combining (1) to (6) it is easy to show that, as expected, the rise speed of the agglomerate increases as the number of attached bubbles is increased. Thus, the maximum rise speed of an agglomerate is limited by the maximum number of bubbles which can attach onto a particle surface. As noted by Matsui *et al*. (1998), the bubbles used during DAF carry a negative surface charge. This negative charge inhibits bubble coalescence by preventing bubbles from approaching too closely to each other, a result which is consistent with the trajectory modelling of Leppinen (1999) who examined the influence of interparticle forces

during DAF. Thus, the bubbles which become attached to a particle should be arranged so that there is some minimum spacing between the bubbles. This suggests that the maximum number of bubbles should depend on the ratio of the surface areas of the particle to the bubbles with

$$i_{\max} = \left\lfloor \max(1, c(d_p / d_b)^2) \right\rfloor \tag{7}$$

where $\lfloor x \rfloor$ is the largest integer less than or equal to x and c is a numerical constant. For fixed bubble and particle sizes, the exact value of c is likely to depend on the electrostatic charges on the surfaces of the bubbles and the particles. Throughout this note, however, the empirical value of $c = 1$ suggested by Matsui *et al.* (1998) will be used.

By using (1) to (7) it is possible to predict the maximum possible rise speed of a bubble/particle agglomerate as a function of the bubble and particle sizes and results are presented in Figure 1 for particles of density $\rho_p = 1.05$ g/cm^3 and bubbles of density $\rho_b = 0.0012$ g/cm^3. The bubbles used during DAF typically range in size from 20–120 μm, and the six curves in Figure 1 correspond to d_b = 20, 40, 60, 80, 100 and 120 μm when looking from bottom to top. The most important observation from the figure is that for each size of bubble there is a global maximum for the rise speed of the bubble/particle agglomerates. This maximum speed increases and occurs at progressively larger particle diameters as the bubble diameter increases. For a fixed bubble size and a fixed particle density greater than that of water, the rise speed of a bubble/particle agglomerate will always become negative (i.e. the agglomerate sinks instead of rising) as the particle becomes sufficiently large. The velocity curves are jagged due to the constraint that an integer number of bubbles must be attached to a particle. For a given number of bubbles attached to a particle, the rise speed decreases as the particle size is increased until the particle surface area has expanded to such an extent that it can accommodate an additional bubble, at which point there is a jump in the maximum achievable rise speed.

It must be stressed that the rise speeds calculated using (1) to (7) and the results presented in Figure 1 do not predict the rise speeds of the bubble/particle agglomerates that are formed during DAF. Rather, the current results only impose an upper bound on the rise speed of the agglomerates. Whether or not this rise speed is achieved depends on the number of bubbles which become attached to a particle, and is thus dependent on the kinematics of the bubble/particle interactions in the contact zone of the flotation tank.

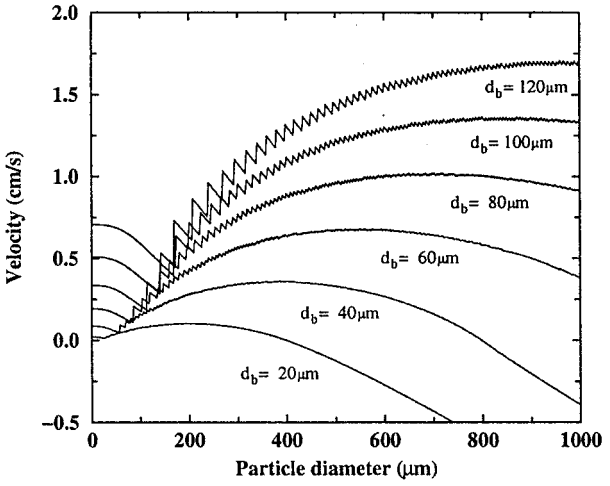

Figure 1 The maximum rise velocity of bubble/particle agglomerates as a function of particle size for bubbles of diameter *db* = 20, 40, 60, 80, 100 and 120 μm when looking from bottom to top

Contact zone modelling

The overall efficiency of a DAF tank is determined by relating the rise speed of the bubble/particle agglomerates leaving the contact zone to the surface loading rate of the tank. If the rise speed of a bubble/particle agglomerate is v_i and the surface loading rate is v_{SL} then overflow theory (Matsui *et al.*, 1998) can be used to calculate the removal fraction, η, as

$$\eta = \min(1, \max(0, v_i / v_{SL})) \tag{8}$$

where η represents the fraction of bubble/particle agglomerates which exit the contact zone and are successfully incorporated into the foam layer at the top of the flotation tank. Thus by developing a model of the formation of bubble/particle agglomerates, (1) to (6) can be combined with (8) in order to determine the global efficiency of flotation.

The formation of bubble/particle agglomerates in the contact zone can be modelled using the population balance approach developed by Matsui *et al.* (1998), which is, in turn, based on the turbulent coagulation theory developed by Saffman and Turner (1956). It is assumed that bubbles collide with particles and bubble/particle agglomerates in the contact zone due to turbulent fluid motion. A bubble/particle agglomerate composed of *i* bubbles and one particle is formed when a bubble collides with, and successfully becomes attached to, a bubble/particle agglomerate which previously contained *i*–1 bubbles. If n_i is the number of particles in the contact zone per unit volume with *i* attached bubbles, then the population balance model can be written as

$$\frac{dn_0}{dt} = -k\alpha_0 n_0 n_{bubbles}, \tag{9}$$

$$\frac{dn_i}{dt} = k\alpha_{i-1} n_{i-1} n_{bubbles} - k\alpha_i n_i n_{bubbles}, \quad i = 1 \text{ to } i_{\max}, \tag{10}$$

where *t* is time, *k* is the turbulent collision rate constant, α_i is the probability that a collision between a bubble and a bubble/particle agglomerate with *i* bubbles will successfully result in the formation of an agglomerate with *i*+1 bubbles, and $n_{bubbles}$ is the number of bubbles per unit volume in the contact zone. Using Saffman and Turner's (1956) turbulent coagulation theory, the collision rate constant is written as

$$k = aG(d_p + d_b)^3 \tag{11}$$

where *a* is a numerical constant, and *G* is a measure of the turbulence intensity with $G=(\varepsilon/\mu)^{1/2}$ where ε is the turbulent dissipation of energy. In solving (9) to (10) it is assumed that $n_{bubbles}$ is so large that it can effectively be treated as a constant (i.e. the incorporation of free bubbles into bubble/particle agglomerates does not significantly reduce the number of free bubbles which remain available for incorporation into subsequent bubble/particle agglomerates). With this assumption $n_{bubbles}$ can be replaced by

$$n_{bubbles} = \frac{\phi}{\pi d_b^3 / 6} \tag{12}$$

where ϕ is the bubble volume concentration in the contact zone.

As noted previously in the section on the rise speed of bubble/particle agglomerates, the bubbles used during DAF carry a negative electrical charge which limits the number of bubbles which can become attached to a single particle. Consequently, Matsui *et al.* (1998) have argued that the bubble adhesion efficiencies (the α_i's), should decrease as the number of bubbles attached to the particle increases. In the Matsui *et al.* (1998) model, α_0, the adhesion efficiency for a bubble-free particle, is assumed to be a constant, while the adhesion

efficiency, α_i, for a particle already having i attached bubbles is given by

$$\alpha_i = \alpha_0\left(1 - i\frac{d_b^2}{d_p^2}\right), \quad i = 1 \text{ to } i_{\max} - 1, \tag{13}$$

$$\alpha_i = 0, \ i = i_{\max}. \tag{14}$$

The value of α_0 depends on the type of particle being floated and is determined empirically.

Substituting (11) to (14) into (9) to (10) gives

$$\frac{dn_0}{dt} = -aG(d_p - d_b)^3 \frac{\phi}{\pi d_b^3 / 6}\alpha_0 n_0, \tag{15}$$

$$\frac{dn_i}{dt} = aG(d_p + d_b)^3 \frac{\phi}{\pi d_b^3 / 6}\left(\left(1 - (i-1)\frac{d_b^2}{d_p^2}\right)n_{i-1} - \left(1 - i\frac{d_b^2}{d_p^2}\right)n_i\right), \ i = 1 \text{ to } i_{\max} - 1, \tag{16}$$

$$\frac{dn_{i\max}}{dt} = aG(d_p + d_b)^3 \frac{\phi}{\pi d_b^3 / 6}\left(1 - (i_{\max} - 1)\frac{d_b^2}{d_p^2}\right)n_{i_{\max}-1}. \tag{17}$$

These equations show the complex dependence of the formation of bubble/particle agglomerates on both the size of the bubbles and the particles. Equations (15) to (17) are solved subject to the initial conditions $n_0 = N_0$ and $n_i = 0$ for all $i \geq 1$, when $t = 0$ in order to determine the values of the n_i after a retention time of $t = t_{contact}$ in the contact zone. Introducing the dimensionless variables $t^* = t/t_{contact}$ and $n_i^* = n_i/N_0$, (15) to (17) become

$$\frac{dn_0^*}{dt^*} = -\kappa n_0^*, \tag{18}$$

$$\frac{dn_i^*}{dt^*} = \kappa\left(\left(1 - (i-1)\frac{d_b^2}{d_p^2}\right)n_{i-1}^* - \left(1 - i\frac{d_b^2}{d_p^2}\right)n_i^*\right), \quad i = 1 \text{ to } i_{\max} - 1, \tag{19}$$

$$\frac{dn_{i_{\max}}^*}{dt^*} = \kappa\left(1 - (i_{\max} - 1)\frac{d_b^2}{d_p^2}\right)n_{i_{\max}-1}^*, \tag{20}$$

where

$$\kappa = 6aGt_{contact}(1 + d_p / d_b)^3 \phi\alpha_0 / \pi \tag{21}$$

is the dimensionless flotation rate constant. The flotation rate constant can be increased by: (1) increasing the level of turbulence in the contact zone to promote more collisions, (2) increasing the time in the contact zone, (3) increasing the number of bubbles in the contact zone by decreasing d_b, (4) increasing the number of bubbles in the contact zone by increasing ϕ and (5) by the appropriate use of coagulants to enhance the efficiency of bubble adhesion.

Matsui *et al.* (1998) have noted that (18) to (20) can be solved using the method of Laplace transforms and they have presented solutions for the specific case when $(d_p/d_b)^2$ is an integer. Their results can readily be extended to non-integer values of $(d_p/d_b)^2$ to give

$$n_i^* = \binom{d_p^2 / d_b^2}{i}\exp(-\kappa t^*)\left(\exp\left(\frac{\kappa t^*}{d_p^2 / d_b^2}\right) - 1\right)^i, \quad i = 0 \text{ to } i_{\max} - 1, \tag{22}$$

and

$$n_{i_{\max}}^* = 1 - \sum_{i=0}^{i_{\max}-1} n_i^*, \tag{23}$$

where the generalized combinatorial is defined for all real values of x and all positive

integers i as

$$\binom{x}{i} = \frac{x(x-1)\,\mathrm{L}\,(x-(i-1))}{i(i-1)\,\mathrm{L}\,(2)(1)}. \tag{24}$$

When i=0, the above expression is defined to be equal to 1. The solution presented by Matsui *et al.* (1998) calculates n_i using (22) for all i from i=0 to $i_{\max}$. When $(d_p/d_b)^2$ is not an integer, n_i cannot be expressed in a simple closed form of the type given by (22). Instead, n_i should be calculated using (23).

Results

Matsui *et al.* (1998) have used the above population balance model to examine the influence of particle size on flotation efficiency for a fixed bubble size of d_b = 50 μm. One of their major findings is that DAF is favoured by the use of larger particles. While smaller particles can be floated under some operating conditions, larger particles should be used as the surface loading rate is increased. The above population balance model will be used to show that bubble size, as well as particle size, has a strong influence on the efficiency of flotation.

The global efficiency of DAF is modelled by combining the results for the rise velocities of bubble/particle agglomerates with the results from the population balance model in order to predict the distribution of the rise velocities of the bubble/particle agglomerates as they leave the contact zone of the DAF tank. The global efficiency is calculated by summing (8) over all the bubble/particle agglomerates to give

$$\eta = \sum_{i=0}^{i_{\max}} n_i^*(t^*=1)\min(1,\max(0, v_i / v_{SL})) \tag{25}$$

The influence of bubble and particle size on flotation efficiency is examined at different surface loading rates in Figure 2, which presents contour plots of η as a function of d_b and d_p. The results correspond to a value of $\kappa/(1+d_p/d_b)^3 = 6aGt_{contact}\phi\alpha_0/\pi = 0.275$ which is obtained using the values of G=10 s^{-1}, $t_{contact}$ = 30 s and α_0 = 0.5 taken from Table 1 of Matsui *et al.* (1998), the value α=0.209 taken from Saffman and Turner (1956), and the value of ϕ=0.0046 recommended by Edzwald (1995). The results in Figure 2 correspond to the flotation of particles with ρ_p = 1.05 g/cm^3 by bubbles with ρ_b = 0.0012 gm/cm^3 in water with ρ = 1.0 g/cm^3.

Figure 2 presents results for surface loading rates ranging from v_{SL} = 0.05 to 0.75 cm/s (1.8 to 27 m/hr) and the global efficiency becomes increasingly dependent on bubble and particle size as the surface loading rate is increased. At the lower surface loading rates flotation is efficient, with η > 0.99, over a broad range of bubble and particle sizes. As the surface loading rate is increased, flotation only remains efficient at progressively larger bubble and particle sizes. While Figure 2 highlights the finding by Matsui *et al.* (1998) that DAF is generally favoured by the use of larger particles, the results indicate that the influence of bubble size cannot be ignored. The current generation of DAF tanks typically operate at a surface loading rate of v_{SL} = 10 m/hr, which corresponds approximately to the results presented in Figure 2(c). At this surface loading rate, flotation is only efficient for bubbles approximately 40 μm in diameter and larger. The overall efficiency of the current generation of flotation tanks is therefore consistent with observation that the average bubble size during flotation is typically 40–60 μm (Edzwald, 1995; Fukushi *et al.*, 1998). For the next generation of DAF tanks, where the surface loading rate is expected to exceed 25 m/hr, the results in Figure 2(f) suggest that new DAF nozzles will have to be designed to produce air bubbles around 100 μm in diameter.

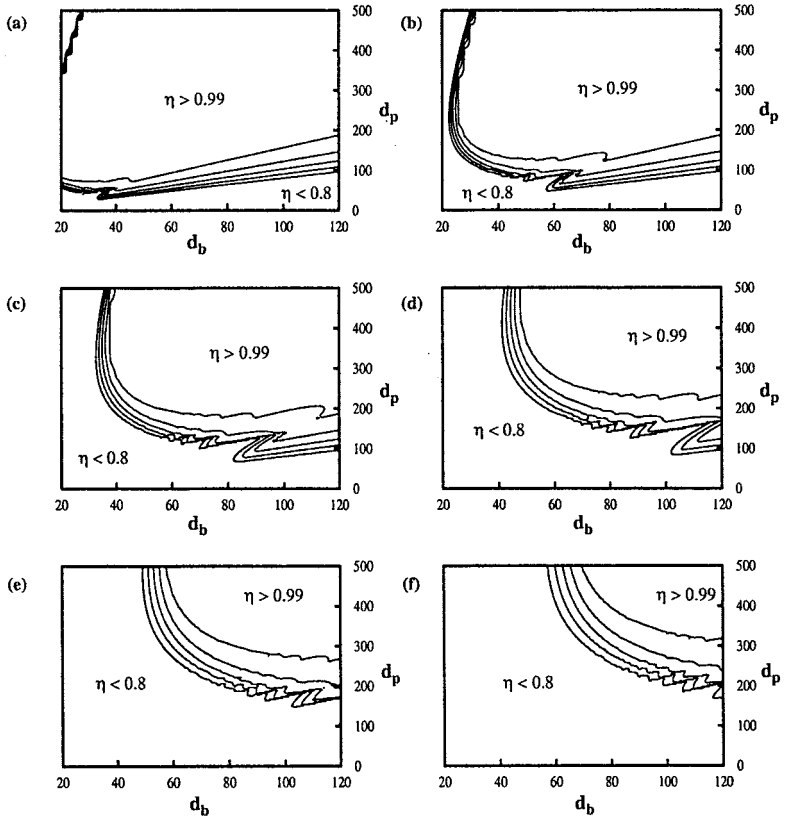

Figure 2 Contour plots of particle removal fraction η for different surface loading rates with (a) v_{SL}=0.05; (b) v_{SL}=0.15; (c) v_{SL}=0.30; (d) v_{SL}=0.45; (e) v_{SL}=0.60; (f) v_{SL}=0.75 cm/s. The contour lines are η = 0.8, 0.85,0.9,0.95 and 0.99 when looking from bottom left to top right

Conclusions

The dependence of particle removal efficiency on bubble and particle size is complex. For fixed bubble size, the maximum possible rise speed of a bubble/particle agglomerate will increase from zero as the particle size, and hence the available surface area for bubble attachment, is increased, until a maximum value is obtained, after which, the rise speed will decrease as the particle size is increased. The rise speed of bubble/particle agglomerates is enhanced to a greater extent by the attachment of larger bubbles, while the kinematics of the attachment process favours the use of smaller bubbles. The attachment process is also enhanced by increasing the level of turbulence in the contact zone of the flotation tank, but this increased turbulence may lead to floc break up which will affect both the kinematics of the attachment process and the rise speeds of the resultant agglomerates. The results presented herein suggest the following conclusion. Flotation efficiency is enhanced by the use of larger particles and larger bubbles. In essence, the added buoyancy due to larger bubbles dominates the kinematics of the bubble attachment process which favours the use of smaller bubbles. The major implication of this finding is that the size of the bubbles used during the DAF stage of potable water production will have to be increased as the new generation of flotation tanks are brought on line. Currently DAF tanks are typically operated at a surface loading rate of 10 m/hr using bubbles which are approximately 50 μm diameter. At the expected surface loading rates of 25 m/hr or more for future DAF tanks, the bubble size will have to be increased by approximately a factor of two. The production of these larger bubbles will require further research into mechanisms for producing an appropriate bubble size

distribution, whether by passing air saturated water through a pressure reduction nozzle, or by some other process.

Acknowledgements

The authors gratefully acknowledge the financial support of Yorkshire Water plc.

References

Clift, R., Grace, J.R. and Weber, M.E. (1978). *Bubbles, Drops and Particles.* Academic Press, London.

Edzwald, J.K. (1995). Principles and applications of dissolved air flotation. *Wat. Sci. Tech.*, **31**(3–4),1–23.

Fukushi, K., Matsui, Y. and Tambo, N. (1998). Dissolved air flotation: experiments and kinetic analysis. *J. Water SRT – Aqua*, **47**, 76–86.

Leppinen, D.M. (1999). Trajectory analysis and collision efficiency during microbubble flotation. *J. Coll. Int. Sci.*, **212**, 431–442.

Matsui, Y., Fukushi, K. and Tambo, N. (1998). Modelling, simulation and operational parameters of dissolved air flotation. *J. Water SRT – Aqua*, **47**, 9–20.

O'Neill, S., Yeung, H. and Oddie, G. (1997). Physical modelling study of the dissolved air flotation process. *Dissolved Air Flotation Technology: an Art or Science*? CIWEM, London, pp 75-86.

Saffman, P.G. and Turner, J.S. (1956). On the collision of drops in turbulent clouds. *J. Fluid Mech.*, **1**, 16–30.

Shawcross, J., Tran, T., Nickols, D. and Ashe, C.R. (1997), Pushing the envelope: dissolved air flotation at ultra-high rate. *Dissolved Air Flotation Technology: an Art or Science*? CIWEM., London, pp 121–139.